

**MATHEMATICAL ENGINEERING
TECHNICAL REPORTS**

**Topology Optimization of Tensegrity
Structures under Compliance Constraint: A
Mixed Integer Linear Programming Approach**

Yoshihiro KANNO

METR 2011-13

April 2011

DEPARTMENT OF MATHEMATICAL INFORMATICS
GRADUATE SCHOOL OF INFORMATION SCIENCE AND TECHNOLOGY
THE UNIVERSITY OF TOKYO
BUNKYO-KU, TOKYO 113-8656, JAPAN

WWW page: <http://www.keisu.t.u-tokyo.ac.jp/research/techrep/index.html>

The METR technical reports are published as a means to ensure timely dissemination of scholarly and technical work on a non-commercial basis. Copyright and all rights therein are maintained by the authors or by other copyright holders, notwithstanding that they have offered their works here electronically. It is understood that all persons copying this information will adhere to the terms and constraints invoked by each author's copyright. These works may not be reposted without the explicit permission of the copyright holder.

Topology Optimization of Tensegrity Structures under Compliance Constraint: A Mixed Integer Linear Programming Approach

Yoshihiro Kanno [†]

*Department of Mathematical Informatics,
University of Tokyo, Tokyo 113-8656, Japan*

Abstract

A tensegrity structure is prestressed pin-jointed structure consisting of discontinuous struts and continuous cables. For exploring new configurations of tensegrity structures, this paper addresses a topology optimization problem of tensegrity structures under the compliance constraint and the stress constraints. It is assumed that a cable loosens and loses the elongation stiffness when its tensile prestress vanishes due to the applied external load. It is shown that the topology optimization problem can be formulated as a mixed integer linear programming (MILP) problem. The proposed method does not require any connectivity information of cables and struts to be known in advance. Numerical experiments illustrate that various configurations of tensegrity structures can be found as the optimal solutions.

Keywords

Tensegrity; Topology optimization; Tension structure; Mixed integer optimization; Complementarity problem; Nonsmooth mechanics.

1 Introduction

The terminology *tensegrity* was coined by Fuller [11] to represent a particular class of tension structures. A tensegrity structure is a prestressed pin-jointed structure consisting of continuous tensile members (cables) and discontinuous compressive members (struts). Many variants of the concept of tensegrity, including so-called tensegrity-like structures, have been presented; see Motro [22] and the references therein.

Tensegrity structures receive remarkable attention from various fields of engineering and science. Light-weight properties and impressive configurations of tensegrity structures are recognized as distinguished advantages in civil engineering structures [2, 5]. Applications of tensegrity structures include deployable structures [33, 35], antenna-mast structures [9], and smart sensors [34]. They are also studied as cell cytoskeleton models [4, 30, 38, 39] and from a view point of discrete mathematics [14].

This paper discusses a topology optimization of tensegrity structures. The topology of a tensegrity structure is characterized by the connectivity of members and the labels indicating

[†]Address: Department of Mathematical Informatics, Graduate School of Information Science and Technology, University of Tokyo, Tokyo 113-8656, Japan. E-mail: kanno@mist.i.u-tokyo.ac.jp. Phone: +81-3-5841-6906, Fax: +81-3-5841-6886.

whether each member is a cable or a strut. A combinatorial feature, stemming from the discontinuity condition of strut, makes finding a new topology of a tensegrity structure an intrinsically difficult problem. To deal with the discontinuity condition of struts rigorously, we develop a *mixed integer linear programming* (MILP) formulation. This approach does not require any information of labels in advance, although the locations of candidate nodes are specified as the input data. Therefore, it is expected that various new topologies can be found as results of optimization.

Since the configuration of a tensegrity structure depends upon the prestresses and any two struts are not allowed to share a common node, an arbitrarily given geometrical configuration is not necessarily realized as a tensegrity structure. Therefore, the determination of the geometrical configuration, called the form-finding process, is a key in the design of a tensegrity structure. Various form-finding methods for tensegrity structures have been proposed by many authors, including [12, 18, 19, 21, 24, 26, 37, 40, 41]; for surveys, see Juan and Mirats Tur [15] and Tibert and Pellegrino [36]. In these methods, it is required to specify the topology of a tensegrity structure as input data.

Based on the group representation theory, it is possible to enumerate topologies of tensegrity structures sharing a common group-symmetry property as shown by Connelly and Back [6] and Connelly and Terrell [7]. Masic *et al.* [19] and Sultan *et al.* [32] proposed form-finding methods for tensegrity structures with a rotational symmetry property,. However, these methods are restricted to finding symmetry tensegrity structures. In contrast, by using the graph representation of the topology and the map L-system, Rieffel *et al.* [29] proposed a form-finding method with a genetic algorithm, which can find asymmetric tensegrity structures. Ehara and Kanno [10] proposed a method based on the ground structure method with MILP, where the topology of tensegrity structures is not required to be specified in advance. However, the mechanical performance of tensegrity structures, e.g., the stiffness or the stability, was not addressed in [10]. Thus form-finding of tensegrity structures without fixing the topology still remains as a challenging problem.

In continuation of the previous work [10], this paper explores the topology optimization of tensegrity structures based on the ground structure method. In addition to the self-equilibrium condition and the discontinuity condition of struts, performance requirements of a tensegrity structure, which were not dealt with in [10], are taken into account. Specifically, we consider the stress constraints and the compliance constraint under the given external load. The minimization problem of the number of cables under these constraints is formulated as an MILP problem, which is solved globally. Note that we assume small deformations and do not consider any stability constraints of tensegrity structures in this paper.

A key idea to formulate our MILP problem for optimization of tensegrity structures is based on the MILP formulations for topology optimization of trusses with discrete member cross-sectional areas [17, 28]. These formulations for trusses are motivated by an MILP formulation for topology optimization of continua presented by Stolpe and Svanberg [31]. Concerning the truss topology optimization with continuous member cross-sectional areas, Ohsaki and Katoh [25] proposed a *mixed integer nonlinear programming* (MINLP) approach. However, as clearly mentioned in Remark 4 of [25], it is not guaranteed that their method finds the global optimal solution. An MINLP approach with the guaranteed global optimality was proposed by Achtziger and Stolpe [1].

A major difference of the static analysis of a tensegrity structure from that of a truss is that some cables may possibly be in slack states at the equilibrium state under the given external load. If we assume the linear elastic material, the constitutive law of a truss element is linear, whereas the axial force of a cable is a nonsmooth function of the elongation. The difficulty of analysis of tensegrity structures stems from the fact that we do not know in advance whether each cable member becomes slack or not at the unknown equilibrium state; see, e.g., [3, 16, 27] for this nonsmoothness property of cables in static equilibrium analysis. Furthermore, in topology optimization of tensegrity structures, it is not determined whether each member is a cable or not in advance. In this paper, we deal with the slack behaviors of cables within the framework of MILP. There are only few literature addressing form-finding or shape-finding problems of cable–strut structures that possibly include slack cables. Deng *et al.* [8] studied the shape-finding problem of cable-strut structures, where some cables become slack during the construction process.

This paper is organized as follows. In section 2, the definition of tensegrity structure is formally stated with a focus on the discontinuity condition of struts. This condition is then reduced to a system of linear inequalities with some 0–1 constraints in section 3. In section 4, the compliance constraint and the stress constraints are formulated as a system of linear inequalities by introducing additional 0–1 variables. Section 5 presents an MILP formulation for topology optimization of tensegrity structures. Numerical examples are demonstrated in section 6 to illustrate that various topologies of tensegrity structures are obtained by the proposed method. Finally, conclusions are drawn in section 7.

A few words regarding our notation: All vectors are assumed to be column vectors. The $(m + n)$ -dimensional column vector $(u^T, v^T)^T$ consisting of $u \in \mathbb{R}^m$ and $v \in \mathbb{R}^n$ is often written as (u, v) for simplicity. We write $p \geq 0$ for $p = (p_i) \in \mathbb{R}^n$ if $p_i \geq 0$ ($i = 1, \dots, n$). For a set E , we use $|E|$ to denote its cardinality. For example, if $E = \{1, \dots, m\}$, then $|E| = m$.

2 Definition of tensegrity structure

Consider a pin-jointed structure without any support as an initial structure for optimization. The members can transmit only axial forces. We assume the small deformation throughout the paper. The members are supposed to consist of a linear elastic material. Each cable is assumed to lose the elongation stiffness when its length becomes shorter than the initial length. This property of a cable is discussed in section 4.

Suppose that the locations of nodes of the structure in the reference configuration are specified in the three-dimensional space. Let V and E denote the set of nodes and the set of members, respectively, where $|V| = n$ and $|E| = m$. For simplicity, we assume $E = \{1, \dots, m\}$ without loss of generality. We use $q = (q_i) \in \mathbb{R}^m$ to denote the vector of axial forces introduced to the members as prestresses. Each member is classified whether a cable or a strut according to prestress q_i ; $q_i > 0$ for a cable and $q_i < 0$ for a strut.

We say that the structure with $q \neq 0$ is at the state of self-equilibrium if it satisfies the static equilibrium condition when no external load is applied. The static equilibrium condition, or the force-balance equation, is written as

$$Hq = 0,$$

where $H \in \mathbb{R}^{3n \times m}$ is the equilibrium matrix.

Among diverse definitions of tensegrity and tensegrity-like structures [22], in this paper attention is focused on the classical one consisting of the self-equilibrium condition and the discontinuity condition of struts. In other words, by a tensegrity structure we mean a pin-jointed prestressed structure, any two struts of which do not share a common node. Let $E(n_j) \subset E$ denote the set of indices of the members that are connected to the node $n_j \in V$. The definition above is formally stated as follows.

Definition 2.1. A structure is said to be a tensegrity structure if there exists $q \in \mathbb{R}^m \setminus \{0\}$ satisfying

$$Hq = 0, \tag{1}$$

$$|\{i \in E(n_j) \mid q_i < 0\}| \leq 1, \quad \forall n_j \in V. \tag{2}$$

■

3 Constraints on self-equilibrium axial forces

The discontinuity condition of struts, i.e., (2), is reduced to a system of linear inequalities with some 0–1 constraints. The lower and upper bound constraints for prestresses are also introduced.

3.1 Labels of members

Within the framework of the conventional ground structure method, we consider a pin-jointed initial structure consisting of sufficiently many candidate members. To realize a tensegrity structure, some members will be removed from this initial structure, while each of the remaining members is determined as either a strut or a cable. More precisely, we attempt to find the partition $\{S, C, N\}$ of E , where S , C , and N are the sets of struts, cables, and removed members, respectively. In other words, S , C , and N are disjoint subsets of E satisfying

$$S \cup C \cup N = E,$$

and member i is labeled as follows:

- The i th member is a strut if $i \in S$.
- The i th member is a cable if $i \in C$.
- The i th member is removed from the structure if $i \in N$.

In accordance with these labels, we next formulate the inequalities which the member axial forces should satisfy. The key idea to do this was first presented by Ehara and Kanno [10], but the formulation is modified to adjust to our present problem in question.

For member i , we introduce two 0–1 variables, x_i and y_i , to represent the label of the member. Specifically, we link $x_i \in \{0, 1\}$ and $y_i \in \{0, 1\}$ to S , C , and N as

$$(x_i, y_i) = (1, 0) \Leftrightarrow i \in S, \tag{3a}$$

$$(x_i, y_i) = (0, 1) \Leftrightarrow i \in C, \tag{3b}$$

$$(x_i, y_i) = (0, 0) \Leftrightarrow i \in N. \tag{3c}$$

The case which is not considered in (3) is excluded, i.e.,

$$(x_i, y_i) \neq (1, 1). \quad (4)$$

From the definitions of a strut and a cable, the prestress q_i satisfies

$$q_i \in \begin{cases}]-\infty, 0[& \text{if } i \in S, \\]0, +\infty[& \text{if } i \in C, \\ \{0\} & \text{if } i \in N. \end{cases} \quad (5)$$

Let M and ϵ be positive constants, where M is sufficiently large and ϵ is sufficiently small, i.e., $0 < \epsilon \ll M$. Then constraint (5) together with (3) and (4) is rewritten as

$$-Mx_i \leq q_i \leq M(1 - x_i) - \epsilon, \quad (6a)$$

$$-M(1 - y_i) + \epsilon \leq q_i \leq My_i, \quad (6b)$$

$$x_i \in \{0, 1\}, \quad (6c)$$

$$y_i \in \{0, 1\}. \quad (6d)$$

We can see that (6) represents conditions (3)–(5) as follows. If $(x_i, y_i) = (1, 0)$, then the second inequality of (6a) reads

$$q_i \leq -\epsilon,$$

which means $i \in S$. Similarly, if $(x_i, y_i) = (0, 1)$, then the first inequality of (6b) reads

$$\epsilon \leq q_i,$$

which means $i \in C$. In the case of $(x_i, y_i) = (0, 0)$, from the first inequality of (6a) and the second inequality of (6b) we obtain

$$0 \leq q_i, \quad q_i \leq 0,$$

which means $i \in N$. Finally, if we put $(x_i, y_i) = (1, 1)$, then the second inequality of (6a) and the first inequality of (6b) are reduced to

$$q_i \leq -\epsilon, \quad \epsilon \leq q_i,$$

which lead the contradiction; thus (6) implies (4).

In this section, we have seen in (6) that the member labels expressed by $(x_i, y_i) \in \{0, 1\}^2$ are linked to the constraints of the member axial forces. This is a fundamental idea to distinguish whether each member belongs to S , C , or N . Note again that in (6) we assume that M is sufficiently large and ϵ is sufficiently small. These crude assumptions will be sharpened in section 3.4 by introducing the practical constraints of the prestresses.

3.2 Discrete cross-sectional areas

Let a_i denote the cross-sectional area of the i th member. It is often that a real-world tensegrity structure consists of struts (and cables, respectively) with unified cross section, where the cross-sectional area of a strut is usually larger than that of a cable; see, e.g., the examples discussed in [2, 23, 35]. Hence, we suppose that the cross-sectional areas for a strut and a cable are specified as ξ_s and ξ_c , respectively, where ξ_s and ξ_c ($\xi_s \geq \xi_c$) are positive constants. In other words, a_i is given by

$$a_i = \begin{cases} \xi_s & \text{if } i \in S, \\ \xi_c & \text{if } i \in C, \\ 0 & \text{if } i \in N. \end{cases} \quad (7)$$

Recall that x_i and y_i serve as the label of the i th member in the sense of (3) when x_i , y_i , and q_i satisfy (6). Therefore, under constraint (6), (7) is equivalently rewritten as

$$a_i = \xi_s x_i + \xi_c y_i. \quad (8)$$

3.3 Initial member lengths

As stated in section 3.1, we adopt the ground structure method for topology optimization of tensegrity structures. As input data of the optimization problem, we specify the locations of the nodes of the ground structure, i.e., the configuration of the structure. It should be clear that this configuration is supposed to be the self-equilibrium configuration compatible with q . In other words, the *initial* configuration before the prestresses q are introduced is unknown. This is a difference of our approach from the conventional ground structure method for trusses.

Since the nodal locations of the ground structure are specified, the length of member i , denoted l_i , is also specified. Note that l_i corresponds to the deformed member length corresponding to the prestress q_i . The initial length, i.e., the undeformed length, is unknown and depends on q_i . In [20], both of the initial member lengths and the self-equilibrium configuration are considered as design variables, while the labels of members are supposed to be specified in advance. In contrast, in our approach, the locations of the nodes in the self-equilibrium configuration are supposed to be given, while the labels of members are considered as design variables.

Let l_i^0 denote the initial length of member i . Since the member length in the deformed state is l_i , the axial force q_i is written as

$$q_i = \frac{Y a_i}{l_i^0} (l_i - l_i^0), \quad (9)$$

where Y is Young's modulus. Once the optimization problem of a tensegrity structure is solved, the prestress q_i and the member cross-sectional area a_i are determined. Then we can compute l_i^0 from (9) as

$$l_i^0 = \frac{Y a_i l_i}{q_i + Y a_i}. \quad (10)$$

Note that the unstressed configuration of the structure defined by $l^0 = (l_i^0 \mid i = 1, \dots, m)$ in (10) is not necessarily connected, although by introducing the prestresses q we can certainly

construct a connected tensegrity structure. This is because we do not consider the compatibility relations between the member elongations and the nodal displacements from the initial unstressed configuration to the prestressed self-equilibrium configuration. In other words, the vector of member elongations, i.e., $l - l^0$, does not necessarily satisfy $(l - l^0) \in \text{Im } H^T$.

3.4 Stress constraints

Let σ_i denote the stress of the i th member. The lower and upper bound constraints for the stress are given by

$$\sigma_i \in \begin{cases} [-\bar{\sigma}_s, -\underline{\sigma}_s] & \text{if } i \in S, \\ [\underline{\sigma}_c, \bar{\sigma}_c] & \text{if } i \in C, \\ \{0\} & \text{if } i \in N, \end{cases} \quad (11)$$

where $\bar{\sigma}_s$, $\underline{\sigma}_s$, $\underline{\sigma}_c$, and $\bar{\sigma}_c$ are positive constants. Since the strut is in compression, we consider the lower bound $-\bar{\sigma}_s < 0$ and the upper bound $-\underline{\sigma}_s < 0$. Similarly, since the cable is in tension, we consider the lower bound $\underline{\sigma}_c > 0$ and the upper bound $\bar{\sigma}_c > 0$.

For simplicity, define \underline{q}_s , \bar{q}_s , \underline{q}_c , and \bar{q}_c by

$$\begin{aligned} \underline{q}_s &= \underline{\sigma}_s \xi_s, & \bar{q}_s &= \bar{\sigma}_s \xi_s, \\ \underline{q}_c &= \underline{\sigma}_c \xi_c, & \bar{q}_c &= \bar{\sigma}_c \xi_c, \end{aligned}$$

which are the lower and upper bounds for the axial forces. Then (11) can be rewritten in terms of q_i as

$$q_i \in \begin{cases} [-\bar{q}_s, -\underline{q}_s] & \text{if } i \in S, \\ [\underline{q}_c, \bar{q}_c] & \text{if } i \in C, \\ \{0\} & \text{if } i \in N. \end{cases} \quad (12)$$

Condition (13) in the following proposition is obtained as a tightened version of (6) in section 3.1 by replacing the constants M and ϵ with specific values related to constraint (12).

Proposition 3.1. *Suppose that (3) holds. Then q_i satisfies (12) if and only if q_i , x_i , and y_i satisfy*

$$-\bar{q}_s x_i \leq q_i \leq (\bar{q}_c + \underline{q}_s)(1 - x_i) - \underline{q}_s, \quad (13a)$$

$$-(\bar{q}_s + \underline{q}_c)(1 - y_i) + \underline{q}_c \leq q_i \leq \bar{q}_c y_i, \quad (13b)$$

$$x_i \in \{0, 1\}, \quad (13c)$$

$$y_i \in \{0, 1\}. \quad (13d)$$

Proof. If $(x_i, y_i) = (1, 0)$, i.e., $i \in S$, then (13a) and (13b) are reduced to

$$\begin{aligned} -\bar{q}_s &\leq q_i \leq -\underline{q}_s, \\ -(\bar{q}_s + \underline{q}_c) + \underline{q}_c &\leq q_i \leq 0. \end{aligned}$$

These inequalities read (12) for $i \in S$. If $(x_i, y_i) = (0, 1)$, i.e., $i \in C$, then (13a) and (13b) are reduced to

$$\begin{aligned} 0 &\leq q_i \leq (\bar{q}_c + \underline{q}_s) - \underline{q}_s, \\ -\underline{q}_c &\leq q_i \leq \bar{q}_c. \end{aligned}$$

These inequalities read (12) for $i \in C$.

In the case of $(x_i, y_i) = (0, 0)$, i.e., $i \in N$, the first inequality of (13a) and the second inequality of (13b) are reduced to $0 \leq q_i$ and $q_i \leq 0$, respectively. These two inequalities implies $q_i = 0$, which is identical to (12) for $i \in N$. Finally, if we put $(x_i, y_i) = (1, 1)$, then the second inequality of (13a) and the first inequality of (13b) are reduced to

$$\begin{aligned} q_i &\leq -\underline{q}_s < 0, \\ 0 &< \underline{q}_c \leq q_i. \end{aligned}$$

Thus a contradiction is led, and hence $(x_i, y_i) \neq (1, 1)$ under constraint (13). \square

Besides the stress constraints given by (13), q should satisfy (1) and (2) in Definition 2.1. Among them, (1) is tractable, because it is a system of linear equations. An intractable one, (2), is discussed in section 3.5.

3.5 Discontinuity condition of struts

The discontinuity condition of struts, which is defined as (2) in Definition 2.1, is an intrinsically difficult condition when we attempt to design a new tensegrity structure. The following proposition shows that this condition is written by using the 0–1 variables x_1, \dots, x_m .

Proposition 3.2. *Suppose that $q = (q_i) \in \mathbb{R}^m$ and $x = (x_i) \in \mathbb{R}^m$ satisfy (13a) and (13c). Then q satisfies (2) if and only if x satisfies*

$$\sum_{i \in E(n_j)} x_i \leq 1, \quad \forall n_j \in V. \quad (14)$$

Proof. Condition (13a) is reduced to

$$-\bar{q}_s x_i \leq q_i \leq -\underline{q}_s$$

if $x_i = 1$, while it is reduced to

$$0 \leq q_i \leq \bar{q}_c$$

if $x_i = 0$. Therefore, (13a) and (13c) imply

$$\begin{aligned} x_i = 1 &\Leftrightarrow i \in S, \\ x_i = 0 &\Leftrightarrow i \in C \cup N, \end{aligned}$$

because S , C , and N are related to q_i as (5). From this observation, we obtain

$$\sum_{i \in E(n_j)} x_i = |\{i \in E(n_j) \mid i \in S\}|,$$

which concludes the proof. \square

A key point of this proof is that $\sum_{i \in E(n_j)} x_i$ is equal to the number of struts connected to the node n_j . It is worth of noting that the total number of cables of the structure becomes equivalent to $\sum_{i \in E} y_i$, when q and y satisfy (13a) and (13c). In section 5.4, we consider the optimization problem to find a tensegrity structure with the minimal number of cables.

3.6 Tensegrity condition under stress constraints

In section 3.2 through section 3.5, we have investigated the conditions which the prestresses q should satisfy so that the structure meets the requirement of the definition of tensegrity, i.e., Definition 2.1, and the upper and lower bound constraints for prestresses. The upshot of this investigation is that (1), (13), and (14) should be satisfied, where $(x_i, y_i) \in \{0, 1\}^2$ playing a role of the label of member i . Under these conditions, the member cross-sectional area is given by (8).

Thus the constraints concerning the self-equilibrium state, i.e., the equilibrium state without external load but with the internal prestresses, have been described completely. In the following section, we will explore the constraints concerning the equilibrium state subjected to the external load.

4 Constraints on compliance

In this section, we explore the compliance constraint, as well as the stress constraints, at the equilibrium state of a tensegrity structure subjected to a static external load. A distinctive feature of a tensegrity structure compared with a conventional truss is that cable members included in a tensegrity structure may possibly become slack at the equilibrium state corresponding to the given external load. Since the internal member forces certainly depend upon the topology, we do not know in advance which members become slack at the (unknown) equilibrium state.

This difficulty is attacked within the framework of MILP. For simplicity of presentation, we begin with the case without prestresses; in section 4.1, we focus on the constitutive laws and the compatibility relations of struts, cables, and removed members. Then section 4.2 shows that the equilibrium conditions and the stress constraints in the presence of the specified prestresses can be formulated as linear inequalities together with some 0–1 constraints. Finally, the compliance constraint is investigated in section 4.3, where the no-compression property of cables is fully addressed.

4.1 Constitutive laws and compatibility relations without prestresses

In this section, we study the constitutive laws and the compatibility relations for the members of a tensegrity structure. For simplicity, we suppose that no prestress is introduced, i.e., $q = 0$. The obtained result is then extended to the case with prestresses in section 4.2.

Let $u \in \mathbb{R}^d$ denote the vector of nodal displacements, where the number of degrees of freedom is $d = 3|V|$. We use c_i to denote the elongation of member i . Then the compatibility relation, which associates c_i with u , is written as

$$c_i = h_i^T u, \quad \forall i \in E. \quad (15)$$

Here, $h_i \in \mathbb{R}^d$ is the i th column vector of the equilibrium matrix H in (1), i.e.,

$$H = [h_1 \mid h_2 \mid \cdots \mid h_m].$$

For member i , we denote by s_i the axial force compatible with the elongation c_i . The elongation stiffness is given by Ea_i/l_i , where a_i is the member cross-sectional area defined by (7), and l_i is the initial member length. When we construct a real-life tensegrity structure, it is often that struts are realized as elastic bars. In such a case, a strut sustains not only compressive forces but also tensile forces. Therefore, we assume for $i \in S$ that the elongation stiffness is $Ea_i/l_i (= E\xi_s/l_i)$ regardless whether it is under compression or tension. In contrast, a cable can sustain only tensile forces, and suddenly loses the elongation stiffness when we attempt to apply a compressive force. We say that a cable is in the taut state if it is stretched with a tensile force, while a cable is in the slack state if it is shrunk without transmitting any forces. Since in this section we assume that there exists no prestress, the transition between the taut state and the slack state occurs when the elongation becomes equal to 0. Therefore, for $i \in C$ the elongation stiffness vanishes if $c_i < 0$, i.e.,

$$\forall i \in C : \quad s_i = \begin{cases} \frac{Y\xi_c}{l_i}c_i & \text{if } c_i \geq 0, \\ 0 & \text{if } c_i < 0, \end{cases} \quad (16)$$

where (7) is used.

By summing up the discussion above, the constitutive law and the compatibility relation for each member $i \in E$ are given as

$$s_i = \begin{cases} k_{si}c_i & \text{if } i \in S, \\ \max\{k_{ci}c_i, 0\} & \text{if } i \in C, \\ 0 & \text{if } i \in N, \end{cases} \quad (17a)$$

$$c_i = h_i^T u, \quad (17b)$$

where k_{si} and k_{ci} are the positive constants defined by

$$k_{si} = \frac{Y}{l_i}\xi_s, \quad k_{ci} = \frac{Y}{l_i}\xi_c.$$

It is not effective to handle (17a) in an optimization algorithm directly, because (17a) involves “if-clauses”. We attempt to deal with (17a) within the framework of MILP. To this end, we reformulate (17) as

$$s_i = k_{si}c_{si} + k_{ci}c_{ci}, \quad (18a)$$

$$Mx_i \geq |c_{si}|, \quad (18b)$$

$$M(1 - x_i) \geq |c_{si} - h_i^T u|, \quad (18c)$$

$$My_i \geq |c_{ci}|, \quad (18d)$$

$$-M(1 - y_i) \leq c_{ci} - h_i^T u \leq M(1 - y_i) + M(1 - z_i), \quad (18e)$$

$$-Mx_i \leq s_i \leq Mz_i, \quad (18f)$$

$$z_i \in \{0, 1\}, \quad (18g)$$

where M is a sufficiently large constant. Note that (18) consists of linear equality constraint (18a), linear inequality constraints (18b)–(18f), and integer constraint (18g). This is a key feature with which we reduce the topology optimization problem of tensegrity structures to an MILP problem in section 5. The equivalence of (17) and (18) is formally stated as follows.

Proposition 4.1. *Suppose that (3) holds. Then (17) is equivalent to (18) in the following sense:*

(i) *Suppose that (u, c_i, s_i) satisfies (17). Define c_{si} , c_{ci} and z_i by*

$$c_{si} = \begin{cases} c_i & \text{if } i \in S, \\ 0 & \text{otherwise,} \end{cases} \quad (19)$$

$$c_{ci} = \begin{cases} c_i & \text{if } i \in \{i \in C \mid c_i \geq 0\}, \\ 0 & \text{otherwise,} \end{cases} \quad (20)$$

$$z_i = \begin{cases} 0 & \text{if } i \in \{i \in C \mid c_i < 0\}, \\ 1 & \text{otherwise.} \end{cases} \quad (21)$$

Then $(u, c_{si}, c_{ci}, s_i, x_i, y_i, z_i)$ satisfies (18).

(ii) *Suppose that $(u, c_{si}, c_{ci}, s_i, x_i, y_i, z_i)$ satisfies (18). Define c_i by (17b). Then (u, c_i, s_i) satisfies (17a).*

Proof. We show the assertion by considering each of the three disjoint cases in (3).

(Case 1): $i \in S$, i.e., $(x_i, y_i) = (1, 0)$. Then (18b)–(18f) are reduced to

$$M \geq |c_{si}|, \quad (22)$$

$$c_{si} = h_i^T u, \quad (23)$$

$$c_{ci} = 0, \quad (24)$$

$$-M \leq c_{ci} - h_i^T u \leq M + M(1 - z_i), \quad (25)$$

$$-M \leq s_i \leq Mz_i. \quad (26)$$

Note that (24) is identical to (20) for $i \in S$. It follows from (17b) and (23) that we obtain $c_{si} = c_i$ and thence (19) for $i \in S$ is satisfied. Then (18a) and (24) read $s_i = k_{si}c_{si} = k_{si}c_i$, which means that (17a) for $i \in S$ is satisfied. By putting $z_i = 1$ and using (24), (25) and (26) are reduced to

$$-M \leq -h_i^T u \leq 2M, \quad (27)$$

$$-M \leq s_i \leq M. \quad (28)$$

With a sufficiently large M , (22), (27), and (28) hold for any u , c_{si} , and s . Therefore, z_i defined by (21) is always feasible for (18).

(Case 2): $i \in C$, i.e., $(x_i, y_i) = (0, 1)$. Then (18b)–(18f) are reduced to

$$c_{si} = 0, \quad (29)$$

$$M \geq |c_{si} - h_i^T u|, \quad (30)$$

$$M \geq |c_{ci}|, \quad (31)$$

$$0 \leq c_{ci} - h_i^T u \leq M(1 - z_i), \quad (32)$$

$$0 \leq s_i \leq Mz_i. \quad (33)$$

Note that (29) is identical to (19) for $i \in C$. Moreover, by using (29), (18a) and (30) are reduced to

$$s_i = k_{ci}c_{ci}, \quad (34)$$

$$M \geq |h_i^T u|. \quad (35)$$

Since M is sufficiently large, (35) (and hence (30) also) is satisfied for any u , while (31) is satisfied for any c_{ci} .

The proof proceeds by considering the two cases, “ $c_i \geq 0$ ” and “ $c_i < 0$ ”. First, suppose $c_i \geq 0$. Then (17a) reads

$$s_i = k_{ci}c_{ci} \geq 0, \quad (36)$$

because $k_{ci} > 0$. From (34) and (40), we obtain

$$c_{ci} = c_i. \quad (37)$$

In accordance with (21), suppose $z_i = 1$. Then (32) and (33) are further reduced to

$$c_{ci} = h_i^T u, \quad (38)$$

$$0 \leq s_i \leq M. \quad (39)$$

(17b) and (37) imply (38), while (36) implies (39). Thus, assertion (i) holds. Conversely, suppose that (32) and (33) are satisfied, and define c_i by (17b). If $s_i > 0$, then (33) is feasible if and only if $z_i = 1$. Accordingly, (32) is reduced to $c_{ci} = h_i^T u$. Moreover, $s_i > 0$ and (34) implies $c_{ci} > 0$. Therefore, from (17b) we obtain $s_i = k_{ci}c_{ci}$ and $c_i > 0$, i.e., (17a) for $i \in \{i \in C \mid c_i > 0\}$. If $s_i = 0$, then (34) implies $c_{ci} = 0$. Since we assume $c_i = h_i^T u \geq 0$, (32) is feasible if and only if $c_i = h_i^T u = 0$. This means that (17a) for $i \in \{i \in C \mid c_i = 0\}$ is satisfied. Consequently, assertion (ii) is obtained.

Alternatively, suppose $c_i < 0$. Then (17a) implies $s_i = 0$. From (34), we obtain

$$c_{ci} = 0. \quad (40)$$

Accordingly, (32) is reduced to

$$0 \leq -c_i \leq M(1 - z_i), \quad (41)$$

which is feasible if and only if $z_i = 0$. Thus assertion (i) is obtained. Conversely, suppose that (32) and (33) are satisfied, and define c_i by (17b). If $c_{ci} > 0$, then (32) and $c_i < 0$ imply $z_i = 0$. From this and (33), we obtain $s_i = 0$, which contradicts (34) and $c_{ci} > 0$. Therefore, $c_{ci} \leq 0$. Then (34) and the first inequality of (33) imply $s_i = 0$, which shows assertion (ii).

(Case 3): $i \in N$, i.e., $(x_i, y_i) = (0, 0)$. Then (18b)–(18f) are reduced to

$$c_{si} = 0, \quad (42)$$

$$M \geq |c_{si} - h_i^T u|, \quad (43)$$

$$c_{ci} = 0, \quad (44)$$

$$-M \leq c_{ci} - h_i^T u \leq M + M(1 - z_i), \quad (45)$$

$$0 \leq s_i \leq Mz_i. \quad (46)$$

From (18a), (42), and (44), we obtain $s_i = 0$. Thus, (17a) for $i \in N$ is satisfied. Moreover, (46) is satisfied for any $z_i \in \{0, 1\}$. Since M is sufficiently large, (43) and (45) are satisfied for any u . \square

Remark 4.2. Besides x_i and y_i which serve as the label of the member type, condition (18) in Proposition 4.1 includes z_i as an additional 0–1 variable. When $i \in C$, z_i serves as an indicator representing whether member i is taut or slack; $z_i = 1$ if cable member i is taut (i.e., $c_i > 0$), while $z_i = 0$ if it is slack (i.e., $c_i < 0$). The formulations (18e)–(18g) involving z_i is derived from the complementarity condition stemming from the constitutive law of the cable member as follows.

For $i \in C$, (17a) reads

$$s_i = \begin{cases} k_{ci}c_i & \text{if } c_i \geq 0, \\ 0 & \text{otherwise.} \end{cases} \quad (47)$$

This means that member i becomes slack if the elongation c_i is negative, while it is taut if $c_i \geq 0$. In other words, the elongation stiffness of a cable is regarded as a nonsmooth function of the elongation. It is known that (47) is equivalently rewritten as

$$s_i = k_{ci}c_{ci}, \quad (48)$$

$$s_i \geq 0, \quad c_{ci} - c_i \geq 0, \quad s_i(c_{ci} - c_i) = 0. \quad (49)$$

More precisely, s_i and c_i satisfy (47) if and only if there exists c_{ci} satisfying (48) and (49); see [16, Chap. 4] for details.

As a key feature, (49) includes the complementarity condition, i.e., $s_i(c_{ci} - c_i) = 0$, that implies that at least one of s_i and $(c_{ci} - c_i)$ is equal to 0. We rewrite this condition as linear inequalities by introducing $z_i \in \{0, 1\}$. Specifically, (49) is equivalent to

$$0 \leq c_{ci} - h_i^T u \leq M(1 - z_i), \quad (50a)$$

$$0 \leq s_i \leq Mz_i, \quad (50b)$$

$$z_i \in \{0, 1\}. \quad (50c)$$

This condition is involved in (18e)–(18g). Indeed, if $i \in C$, i.e., $(x_i, y_i) = (0, 1)$, then (18e)–(18g) are reduced to (50). \blacksquare

Remark 4.3. Proposition 4.1 does not assert that every solution $(u, c_{si}, c_{ci}, s_i, x_i, y_i, z_i)$ to (18) satisfies (21). Indeed, $z_i = 0$ is also feasible for (18) if $i \in C$ and $c_i = 0$. Moreover, if $i \in S \cup N$, then $z_i = 0$ is feasible. In section 5.3, we introduce a valid inequality to exclude $z_i = 0$ ($i \in S \cup N$) from the solution set of (18). \blacksquare

4.2 Stress constraints at equilibrium state subjected to external load

Under the assumption of nonexistence of prestresses, section 4.1 have shown that the constitutive laws and the compatibility relations of a tensegrity structure can be formulated as a system of linear inequalities with some integer constraints. In this section, we explore the equilibrium condition and the stress constraints in the presence of the prestresses and the external nodal forces. Note that the prestresses q are supposed to satisfy the constraints in section 3.6.

Recall that we have studied the self-equilibrium condition in section 3 for a free-standing tensegrity structure, i.e., a tensegrity structure without supports. To introduce the compliance constraint as a performance requirement, we suppose that some degrees of freedom of the displacements are fixed by pin-supports so that the tensegrity structure can be in equilibrium under an arbitrarily given external load. Consider a partition $J_N \cup J_D = \{1, \dots, d\}$ of the set of indices of the degrees of freedom of displacements. Then the external force for each $j \in J_N$ is supposed to be specified as f_j , while the displacement for each $j \in J_D$ is prescribed to be equal to 0.

As mentioned in section 3.3, the given configuration of the ground structure corresponds to the self-equilibrium state in the presence of the prestresses q . Then we apply the specified external forces f_j ($j \in J_N$), while the displacements of the supports are restricted as $u_j = 0$ ($j \in J_D$). To be in equilibrium, the tensegrity structure is deformed from the self-equilibrium configuration. The attained equilibrium state is simply called the equilibrium state in what follows. We denote by s the vector of axial forces equilibrate with the external load f_j ($j \in J_N$), while the vector of nodal displacements from the self-equilibrium configuration is denoted by u . Accordingly, s_i is compatible with the elongation $c_i = h_i^T u$. We use \tilde{s}_i to denote the total axial force at the equilibrium state, i.e.,

$$\tilde{s}_i = q_i + s_i. \quad (51)$$

For $i \in C$, the cable member i is taut if $\tilde{s}_i > 0$, while $\tilde{s}_i = 0$ if the member is slack. If $i \in S$, then member i can transmit both compressive and tensile forces, as discussed in section 4.1. For $i \in N$, we have $\tilde{s}_i = 0$. Therefore, the constitutive law and the compatibility relation for each member $i \in E$ are given by

$$s_i = \begin{cases} k_{si} c_i & \text{if } i \in S, \\ \max\{k_{ci} c_i, -q_i\} & \text{if } i \in C, \\ 0 & \text{if } i \in N, \end{cases} \quad (52a)$$

$$c_i = h_i^T u. \quad (52b)$$

The force-balance equation and the kinematic constraints of the prescribed displacements are written as

$$(Hs)_j = f_j, \quad \forall j \in J_N, \quad (53)$$

$$u_j = 0, \quad \forall j \in J_D. \quad (54)$$

From a practical point of view, we shall impose the lower and upper bound constraints on \tilde{s}_i 's. This issue is postponed to (61). We begin by rewriting (52) as a system of linear inequalities with some integer constraints. This is performed in the following proposition, which can be obtained as a slight extension of Proposition 4.1.

Proposition 4.4. *Suppose that (3) holds. Then (52) is equivalent to*

$$s_i = k_{si}c_{si} + k_{ci}c_{ci}, \quad (55a)$$

$$-Mx_i \leq c_{si} \leq Mx_i, \quad (55b)$$

$$M(1 - x_i) \geq |c_{si} - h_i^T u|, \quad (55c)$$

$$-My_i \leq c_{ci} \leq My_i, \quad (55d)$$

$$-M(1 - y_i) \leq c_{ci} - h_i^T u \leq M(1 - y_i) + M(1 - z_i), \quad (55e)$$

$$-Mx_i \leq q_i + k_{ci}c_{ci} \leq Mz_i, \quad (55f)$$

$$z_i \in \{0, 1\} \quad (55g)$$

in the following sense:

(i) *Suppose that (u, c_i, s_i) satisfies (52). Define c_{si} , c_{ci} and z_i by*

$$c_{si} = \begin{cases} c_i & \text{if } i \in S, \\ 0 & \text{otherwise,} \end{cases} \quad (56)$$

$$c_{ci} = \begin{cases} c_i & \text{if } i \in \{i \in C \mid c_i \geq -q_i/k_c\}, \\ 0 & \text{otherwise,} \end{cases} \quad (57)$$

$$z_i = \begin{cases} 0 & \text{if } i \in \{i \in C \mid c_i < -q_i/k_c\}, \\ 1 & \text{otherwise.} \end{cases} \quad (58)$$

Then $(u, c_{si}, c_{ci}, s_i, x_i, y_i, z_i)$ satisfies (55).

(ii) *Suppose that $(u, c_{si}, c_{ci}, s_i, x_i, y_i, z_i)$ satisfies (55). Define c_i by (52b). Then (u, c_i, s_i) satisfies (52a).*

Proof. The proof is analogous to Proposition 4.1 and hence is omitted. \square

In (55) of Proposition 4.4, c_{si} corresponds to the elongation of a strut, while c_{ci} represents the elastic elongation of a cable, i.e., $c_{ci} = s_i/k_{ci}$ if $i \in C$. The following result is obtained as an immediate consequence of Proposition 4.4.

Corollary 4.5. *Suppose that $(u, c_{si}, c_{ci}, s_i, x_i, y_i, z_i)$ satisfies (52). Then,*

$$k_{si}c_{si} = \begin{cases} s_i & \text{if } i \in S, \\ 0 & \text{if } i \in C \cup N, \end{cases} \quad (59)$$

$$k_{ci}c_{ci} = \begin{cases} s_i & \text{if } i \in C, \\ 0 & \text{if } i \in S \cup N. \end{cases} \quad (60)$$

Proof. This assertion follows from (52a), (56), and (57). \square

We next introduce the lower and upper bound constraints on the member stresses at the equilibrium state subjected to the external load. Specifically, the following constraints are imposed on \tilde{s}_i defined by (51):

$$q_i + s_i \in \begin{cases} [-\tilde{s}_s^{\text{lb}}, \tilde{s}_s^{\text{ub}}] & \text{if } i \in S, \\ [0, \tilde{s}_c^{\text{ub}}] & \text{if } i \in C, \end{cases} \quad (61)$$

where \tilde{s}_s^{lb} , \tilde{s}_s^{ub} , and \tilde{s}_c^{ub} are constants satisfying

$$\tilde{s}_s^{\text{lb}} > 0, \quad \tilde{s}_s^{\text{ub}} \geq \bar{q}_c, \quad \tilde{s}_c^{\text{ub}} > 0. \quad (62)$$

Note that s_i in (61) is defined by (52a). By using x_i and y_i , constraint (61) in terms of q_i and \tilde{s}_i can be reduced to the constraints in terms of q_i , c_{si} , and c_{ci} as follows.

Proposition 4.6. *Suppose that (x_i, y_i) satisfies (3), that q_i satisfies (12), and that (c_{si}, c_{ci}) satisfies (59) and (60). Then (q_i, s_i) satisfies (61) if and only if (q_i, c_{si}, c_{ci}) satisfies*

$$-\tilde{s}_s^{\text{lb}} \leq q_i + k_{si}c_{si} \leq \tilde{s}_s^{\text{ub}}, \quad (63)$$

$$-\bar{q}_s x_i \leq q_i + k_{ci}c_{ci} \leq \tilde{s}_c^{\text{ub}}. \quad (64)$$

Proof. By using (59), (63) is reduced to

$$-\tilde{s}_s^{\text{lb}} \leq q_i + s_i \leq \tilde{s}_s^{\text{ub}} \quad \text{if } i \in S, \quad (65a)$$

$$-\tilde{s}_s^{\text{lb}} \leq q_i \leq \tilde{s}_s^{\text{ub}} \quad \text{if } i \in C \cup N. \quad (65b)$$

Observe that (65b) is redundant for $i \in C \cup N$ when q_i satisfies (12) and \tilde{s}_s^{ub} satisfies (62). Moreover, (61) for $i \in S$ is identical to (65a).

By using (3) and (60), (64) is reduced to

$$-\bar{q}_s \leq q_i \leq \tilde{s}_c^{\text{ub}} \quad \text{if } i \in S, \quad (66a)$$

$$0 \leq q_i + s_i \leq \tilde{s}_c^{\text{ub}} \quad \text{if } i \in C, \quad (66b)$$

$$0 \leq q_i \leq \tilde{s}_c^{\text{ub}} \quad \text{if } i \in N. \quad (66c)$$

Here, (66a) is redundant, because (12) for $i \in S$ reads $-\bar{q}_s \leq q_i \leq -\underline{q}_s$, where $-\underline{q}_s < 0 < \tilde{s}_c^{\text{ub}}$. Similarly, (66c) is redundant, because (12) for $i \in N$ reads $q_i = 0$. Moreover, (66b) is identical to (61) for $i \in C$. \square

Remark 4.7. Among the inequalities investigated in Proposition 4.6, we focus on (64) that has a form similar to (55f). Observe that (55f) is reduced to

$$-M \leq q_i + k_{ci}c_{ci} \leq M$$

if $x_i = 1$ and $z_i = 1$. We have assumed that M is sufficiently large so that $q_i + k_{ci}c_{ci}$ can take any value, because in (55f) the lower and upper bound constraints for \tilde{s}_i , i.e., (61), was not considered there. When we impose (61) together with (55), the bound M in (55f) can be tightened by using (64) as

$$-\bar{q}_s x_i \leq q_i + k_{ci}c_{ci} \leq \tilde{s}_c^{\text{ub}} z_i. \quad (67)$$

Instead of (55f) and (64), we consider the constraint (67) to formulate the optimization problem of tensegrity structures in section 5.4. \blacksquare

Remark 4.8. In (52) and (61), the constraints on the stress (or the axial force) are not considered for $i \in N$. Indeed, for $i \in N$, the elongation $h_i^T u$ can take any value. Thus the stress constraints are considered only for the existing members. \blacksquare

Corollary 4.5 implies that (52) implies (59) and (60). Hence, Proposition 4.6 guarantees that (61) is equivalent to (63) and (64) when the variables are subjected to (12) and (52).

We next investigate M in (55b) and (55d). By using the bounds in (12) and (61) for q_i and \tilde{s}_i , the value M for c_{si} and c_{ci} can be tightened based upon the following fact.

Proposition 4.9. *Suppose that (x_i, y_i) satisfies (3), that q_i satisfies (12), and that (c_{si}, c_{ci}) satisfies (59), (60), (63), and (64). Then (c_{si}, c_{ci}) satisfies*

$$-\tilde{s}_s^{\text{lb}} + \underline{q}_s \leq k_{si}c_{si} \leq \tilde{s}_s^{\text{ub}} + \bar{q}_s, \quad (68)$$

$$-\bar{q}_c \leq k_{ci}c_{ci} \leq \tilde{s}_c^{\text{ub}} - \underline{q}_c. \quad (69)$$

Proof. For $i \in S$, (12) is explicitly written as

$$-\bar{q}_s \leq q_i \leq -\underline{q}_s \quad \text{if } i \in S, \quad (70)$$

while, by using (59), (63) is reduced to

$$-\tilde{s}_s^{\text{lb}} \leq q_i + k_{si}c_{si} \leq \tilde{s}_s^{\text{ub}} \quad \text{if } i \in S. \quad (71)$$

It is easy to see that (68) is a necessary condition for (70) and (71). Alternatively, for $i \in C \cup N$, we obtain $c_{si} = 0$ from (59) and thence (68) is always satisfied.

For $i \in C$, (12) is explicitly written as

$$\underline{q}_c \leq q_i \leq \bar{q}_c \quad \text{if } i \in C, \quad (72)$$

while, by using (3) and (60), (64) is reduced to

$$0 \leq q_i + k_{ci}c_{ci} \leq \tilde{s}_c^{\text{ub}} \quad \text{if } i \in C. \quad (73)$$

It is immediate to see that (69) is a necessary condition for (72) and (73). Alternatively, for $i \in S \cup N$, we obtain $c_{ci} = 0$ from (60), and hence (69) is always satisfied. \square

Proposition 4.9 asserts that (55b) can be tightened as

$$(-\tilde{s}_s^{\text{lb}} + \underline{q}_s)x_i \leq k_{si}c_{si} \leq (\tilde{s}_s^{\text{ub}} + \bar{q}_s)x_i, \quad (74)$$

while (55d) can be tightened as

$$-\bar{q}_c y_i \leq k_{ci}c_{ci} \leq (\tilde{s}_c^{\text{ub}} - \underline{q}_c)y_i. \quad (75)$$

4.3 Compliance constraint under external load

In section 4.1 and section 4.2, we have investigated the equilibrium conditions as well as the performance constraints of a tensegrity structure, when the external load exists together with the prestresses.

The governing equations of the equilibrium subjected to the external load f_j ($j \in J_N$) are given by (52), (53), and (54). Note again that u satisfying these governing equations represents the nodal displacements from the self-equilibrium configuration. We consider the constraint of the compliance corresponding to u . In other words, we introduce the upper bound constraint on

the external work done only by f_j ($j \in J_N$). The internal work due to the prestresses q is not constrained in the compliance constraint. Then the compliance, denoted by w , is written as

$$w = \sum_{j \in J_N} f_j u_j.$$

We use \bar{w} to denote the upper bound on w , and hence the compliance constraint is written as

$$\sum_{j \in J_N} f_j u_j \leq \bar{w}. \quad (76)$$

We are now in position to sum up all the constraints for optimization of tensegrity structures. From the definition of tensegrity, the prestresses q should satisfy (1), (2), and (5), when no external load is applied. The lower and upper bound constraints on q are given by (12). Under the external load f_j ($j \in J_N$), the governing equations of equilibrium are written as (52), (53), and (54). At this equilibrium state, the lower and upper bound constraints on the member axial forces are given as (61), while the compliance constraint is given as (76). Thus the constraints which we consider are listed as

$$\sum_{j \in J_N} f_j u_j \leq \bar{w}, \quad (77a)$$

$$(Hs)_j = f_j, \quad \forall j \in J_N, \quad (77b)$$

$$u_j = 0, \quad \forall j \in J_D, \quad (77c)$$

$$s_i = \begin{cases} k_{si} c_i & \text{if } i \in S, \\ \max\{k_{ci} c_i, -q_i\} & \text{if } i \in C, \\ 0 & \text{if } i \in N, \end{cases} \quad \forall i \in E, \quad (77d)$$

$$c_i = h_i^T u, \quad \forall i \in E, \quad (77e)$$

$$q_i + s_i \in \begin{cases} [-\tilde{s}_s^{\text{lb}}, \tilde{s}_s^{\text{ub}}] & \text{if } i \in S, \\ [0, \tilde{s}_c^{\text{ub}}] & \text{if } i \in C, \end{cases} \quad \forall i \in E, \quad (77f)$$

$$q, S, C, \text{ and } N \text{ satisfy (1), (2), and (12)}. \quad (77g)$$

Among these conditions, (77g) have been explored in section 3. Moreover, (77a), (77b), and (77c) are tractable, because they are linear constraints. The subject of section 4.1 and section 4.2 is to reformulate (77d), (77e), and (77f) by making use of discrete variables $x, y, z \in \{0, 1\}^m$. The fundamental idea to reformulate (77d) is presented in Proposition 4.4. Proposition 4.6 and Remark 4.7 deal with (77e). Some inequalities in Proposition 4.4 are tightened using Proposition 4.9 as (74) and (75). The upshot is that (77) is equivalent to the following condition:

$$\sum_{j \in J_N} f_j u_j \leq \bar{w}, \quad (78a)$$

$$(Hs)_j = f_j, \quad \forall j \in J_N, \quad (78b)$$

$$u_j = 0, \quad \forall j \in J_D, \quad (78c)$$

$$s_i = k_{si}c_{si} + k_{ci}c_{ci}, \quad \forall i \in E, \quad (78d)$$

$$(-\tilde{s}_s^{\text{lb}} + \underline{q}_s)x_i \leq k_{si}c_{si} \leq (\tilde{s}_s^{\text{ub}} + \bar{q}_s)x_i, \quad \forall i \in E, \quad (78e)$$

$$M(1 - x_i) \geq |c_{si} - h_i^T u|, \quad \forall i \in E, \quad (78f)$$

$$-\bar{q}_c y_i \leq k_{ci}c_{ci} \leq (\tilde{s}_c^{\text{ub}} - \underline{q}_c)y_i, \quad \forall i \in E, \quad (78g)$$

$$-M(1 - y_i) \leq c_{ci} - h_i^T u \leq M(1 - y_i) + M(1 - z_i), \quad \forall i \in E, \quad (78h)$$

$$-\tilde{s}_s^{\text{lb}} \leq q_i + k_{si}c_{si} \leq \tilde{s}_s^{\text{ub}}, \quad \forall i \in E, \quad (78i)$$

$$-\bar{q}_s x_i \leq q_i + k_{ci}c_{ci} \leq \tilde{s}_c^{\text{ub}} z_i, \quad \forall i \in E, \quad (78j)$$

$$x, y, \text{ and } q \text{ satisfy (1), (13), and (14).} \quad (78k)$$

5 Mixed integer linear programming formulation of tensegrity optimization

This section presents an MILP problem for optimization of tensegrity structures based on the results of section 3 and section 4. It has been shown that the constraints concerning mechanical behaviors of a tensegrity structure are formulated as (78). As constraints required in a practical situation, the constraint excluding intersecting members is discussed in section 5.1, while the constraint avoiding nodes connected only to cables is considered in section 5.2. Section 5.3 discusses valid inequalities in terms of the 0–1 variables. As a consequence, section 5.4 presents an MILP problem for topology optimization of tensegrity structures.

5.1 Practical constraints (1): avoiding intersecting members

In the ground structure method, it is often that an initial structure includes many intersecting candidate members; see for instance Figure 1 in section 6.1. This is because we need to prepare sufficiently large number of candidate members for seeking the optimal topology. For constructing a real-life structure, however, intersecting of existing members, that are chosen from the candidate members, is not accepted. This section discusses the constraints for excluding such intersecting members.

In the problem of optimization of tensegrity structures, existing members are chosen from E , where each existing member is whether a strut or a cable. Therefore, any existing member is included in $S \cup C$, and any two existing members should not intersect. Let P_{cross} denote the set of pairs of intersecting members; we write $(i, i') \in P_{\text{cross}}$ if member i and member i' intersect. Then the constraint excluding intersecting members is formally written as

$$\{i, i'\} \not\subseteq S \cup C, \quad \forall (i, i') \in P_{\text{cross}}. \quad (79)$$

Remark 5.1. Rigorously speaking, two members intersect if the distance of these members is equal to zero. From a practical point of view, existence of too close members is also unacceptable. Therefore, we specify a threshold $\delta > 0$ and let $(i, i') \in P_{\text{cross}}$ if the distance of two line segments representing member i and member i' is not less than δ . ■

Suppose that $i \in S \cup C$ and $(i, i') \in P_{\text{cross}}$. Then (79) requires $i' \in N$. From (3), this relation is written in terms of x and y as

$$x_i = 1 \text{ or } y_i = 1 \quad \Rightarrow \quad x_{i'} = y_{i'} = 0.$$

On the other hand, if $i' \in S \cup C$, then $x_i = y_i = 0$ should be satisfied. Since x_i and y_i cannot be equal to one simultaneously, at most one of $x_i, y_i, x_{i'}$, and $y_{i'}$ can be equal to one. Thus, (79) is equivalently rewritten as

$$x_i + x_{i'} + y_i + y_{i'} \leq 1, \quad \forall (i, i') \in P_{\text{cross}}. \quad (80)$$

5.2 Practical constraints (2): avoiding nodes connected to cables only

It is usual that an actually-constructed tensegrity structure does not have a node connected only to cables, although such a node is not forbidden by Definition 2.1. In this section, we formulate a system of linear inequalities to avoid existence of such nodes.

For node n_j ($n_j \in V$), this constraint is formally stated as follows: if there exists at least one member connecting to n_j , then there should exist a strut connecting to n_j . The contraposition of this statement is written as

$$S \cap E(n_j) = \emptyset \quad \Rightarrow \quad C \cap E(n_j) = \emptyset$$

for each $n_j \in V$. By using (3), this relation is written in terms of x_i and y_i as

$$\sum_{i \in E(n_j)} x_i = 0 \quad \Rightarrow \quad y_i = 0 \quad (\forall i \in E(n_j)).$$

This condition can be rewritten as

$$y_i \leq \sum_{i' \in E(n_j)} x_{i'}, \quad \forall i \in E(n_j). \quad (81)$$

5.3 Valid inequalities

When we solve an MILP problem with a branch-and-bound or a branch-and-cut algorithm, it is often that adding valid inequalities to the constraints of the MILP problem improves the computational efficiency. This section concerns some valid inequalities in terms of the integer variables x_i, y_i , and z_i .

The first one stems from (3) and (4). Since $(x_i, y_i) \in \{0, 1\}^2$, (3) is rewritten as

$$x_i + y_i \leq 1. \quad (82)$$

On the other hand, we have seen in the proof of Proposition 3.1 that (13) (and hence (78) also) implies (4). Therefore, (82) works as a valid inequality.

The second valid inequality stems from Proposition 4.4 (i); see Remark 4.3 also. It follows from (58) that we can fix $z_i = 1$ if $i \notin C$, i.e., if $y_i = 0$. Therefore, we can add

$$y_i + z_i \geq 1 \tag{83}$$

to (78) as a valid inequality.

5.4 MILP formulation

We are now in position to formulate the optimization problem of tensegrity structures. Recall that the constraints for mechanical responses of tensegrity structures are formulated as (78) in section 4.3. We also consider (80) in section 5.1 and (81) in section 5.2 as constraints of practical requirements. Furthermore, the valid inequalities, (82) and (83) in section 5.3, are incorporated.

We may consider some different objective functions; see Remark 5.2. Among them, we focus on the minimization problem of the number of cables, i.e., $|C| = \sum_{i=1}^m y_i$ for the following reasons. Suppose that the number of struts is fixed for simplicity. Then, roughly speaking, the larger the number of cables, the larger the degree of static indeterminacy. Hence, the number of self-equilibrium modes of the axial forces also increases if the number of cables increases. Among these self-equilibrium modes, if at least one mode satisfies the discontinuity condition of struts, then the structure is regarded as a tensegrity structure according to Definition 2.1. Therefore, finding a tensegrity structure with the smallest number of cables, called the *minimal tensegrity structure* in [10], is a challenging problem, compared with finding a tensegrity structure with many cables. Moreover, the minimal tensegrity structure is certainly the simplest structure in the sense that we cannot remove any cables without removing some struts. Many of existing tensegrity structures give somehow fragile impression, that seem to attract the interest of people. Such a tensegrity structure consists of relatively few cables compared with the number of struts. These reasons motivate us to attempt to find the tensegrity structure with the minimum number of cables.

Consequently, the optimization problem of tensegrity structures is formulated as the following

MILP problem:

$$\begin{aligned}
& \min_{x,y,z,q,s,c_s,c_c,u} \sum_{i \in E} y_i \\
\text{s. t.} \quad & Hq = 0, \\
& -\bar{q}_s x_i \leq q_i \leq (\bar{q}_c + \underline{q}_s)(1 - x_i) - \underline{q}_s, & \forall i, \\
& -(\bar{q}_s + \underline{q}_c)(1 - y_i) + \underline{q}_c \leq q_i \leq \bar{q}_c y_i, & \forall i, \\
& \sum_{i \in E(n_j)} x_i \leq 1, & \forall n_j \in V, \\
& x_i + x_{i'} + y_i + y_{i'} \leq 1, & \forall (i, i') \in P_{\text{cross}}, \\
& y_i \leq \sum_{i' \in E(n_j)} x_{i'}, \quad \forall i \in E(n_j), & \forall n_j \in V, \\
& \sum_{j \in J_N} f_j u_j \leq \bar{w}, & \\
& (Hs)_j = f_j, & \forall j \in J_N, \\
& u_j = 0, & \forall j \in J_D, \\
& s_i = k_{si} c_{si} + k_{ci} c_{ci}, & \forall i, \\
& (-\tilde{s}_s^{\text{lb}} + \underline{q}_s) x_i \leq k_{si} c_{si} \leq (\tilde{s}_s^{\text{ub}} + \bar{q}_s) x_i, & \forall i, \\
& M(1 - x_i) \geq |c_{si} - h_i^T u|, & \forall i, \\
& -\bar{q}_c y_i \leq k_{ci} c_{ci} \leq (\tilde{s}_c^{\text{ub}} - \underline{q}_c) y_i, & \forall i, \\
& -M(1 - y_i) \leq c_{ci} - h_i^T u \leq M(2 - y_i - z_i), & \forall i, \\
& -\tilde{s}_s^{\text{lb}} \leq q_i + k_{si} c_{si} \leq \tilde{s}_s^{\text{ub}}, & \forall i, \\
& -\bar{q}_s x_i \leq q_i + k_{ci} c_{ci} \leq \tilde{s}_c^{\text{ub}} z_i, & \forall i, \\
& x_i + y_i \leq 1, & \forall i, \\
& y_i + z_i \geq 1, & \forall i, \\
& x_i \in \{0, 1\}, \quad y_i \in \{0, 1\}, \quad z_i \in \{0, 1\}, & \forall i.
\end{aligned} \tag{84}$$

In this problem, continuous variables are q , s , c_s , c_c , and u , while binary variables are x , y , and z . All the constraints other than the integer constraints are linear constraints. Thus, problem (84) is a 0–1 mixed integer linear programming problem, and hence it can be solved globally by using, e.g., a branch-and-cut algorithm. Several software packages, e.g., CPLEX [13], are available for this purpose.

Remark 5.2. In problem (84), we attempt to minimize the number of cables. Several different objective functions can be considered. For example, the minimization problem of the structural volume, which is usually considered in optimization of trusses, can also be formulated as an MILP problem. Since the member cross-sectional area is given by (7), the structural volume, denoted v , can be written as

$$v = \sum_{i=1}^m \xi_s l_i x_i + \sum_{i=1}^m \xi_c l_i y_i.$$

By replacing the objective function of problem (84) with v , we obtain an MILP formulation of the minimization problem of the structural volume. ■

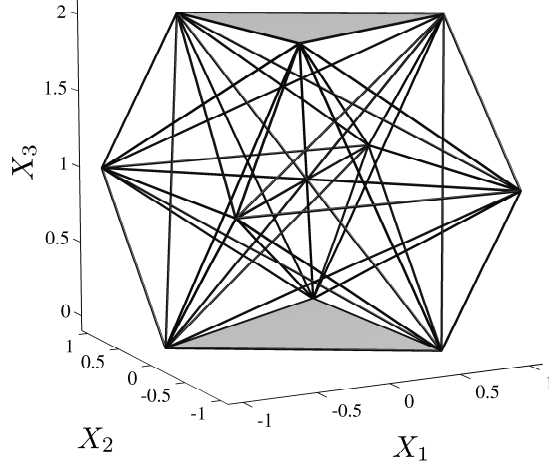


Figure 1: An initial structure with three layers.

6 Numerical experiments

The optimal topologies of various tensegrity structures are computed by solving problem (84). Computation was carried out on Quad-Core Xeon E5450 (3 GHz) with 16 GB RAM. The MILP problems were solved by using CPLEX Ver. 11.2 [13] with the default settings.

6.1 Three-layer tensegrity structures

Consider an initial structure illustrated in Figure 1. The structure consists of $|V| = 10$ nodes and $|E| = 45$ members, where any two nodes are connected by a member. The nodes form three horizontal layers. In Figure 1, the top and bottom layers are shaded, X_1 and X_2 are taken to be two horizontal axes, and the vertical axis is denoted by X_3 . The top and bottom layers are in equilateral triangular shapes, while the middle one is in a square shape. The length of an edge of the equilateral triangle is $\sqrt{3}$ m, while that of the square is $1.4\sqrt{2}$ m. An edge of each triangle and two edges of the square are parallel with the X_2 -axis. The centers of these three layers are located at $(0,0,0)$, $(0,0,1)$, and $(0,0,2)$, and hence the distance between the square and each triangle is 1.0 m.

6.1.1 Setting of parameters

The Young modulus of each member is $Y = 1.0$ GPa. The member cross-sectional areas of a strut and a cable are $\xi_s = 1000.0$ mm² and $\xi_c = 100.0$ mm², respectively. The lower and upper bounds for member stresses in (11) are $\underline{\sigma}_s = 0.1$ MPa, $\bar{\sigma}_s = 2.0$ MPa, $\underline{\sigma}_c = 0.5$ MPa, and $\bar{\sigma}_c = 10.0$ MPa. Therefore, the bounds for q_i in (12) are $\underline{q}_s = 0.1$ kN, $\bar{q}_s = 2.0$ kN, $\underline{q}_c = 0.05$ kN, and $\bar{q}_c = 1.0$ kN. The bounds for $\tilde{s}_i = q_i + s_i$ in (61) are chosen as $\tilde{s}_s^{\text{lb}} = \bar{q}_c$, $\tilde{s}_s^{\text{ub}} = \bar{q}_c$, and $\tilde{s}_c^{\text{ub}} = \bar{q}_c$. As J_D , six degrees of displacements of the bottom nodes are fixed to avoid the rigid body motion. Specifically, we fix the displacements in all directions of the node at $(1/2, \sqrt{3}/2, 0)$, the displacements in the X_1 and X_3 directions of the node at $(-1, 0, 0)$, and the displacement in the X_3 direction of the node at $(1/2, -\sqrt{3}/2, 0)$. As stated in Remark 5.1, the threshold δ is used to define P_{cross} . We choose $\delta = 5.0 \times 10^2$ m, which results in $|P_{\text{cross}}| = 14$; i.e., there are 14

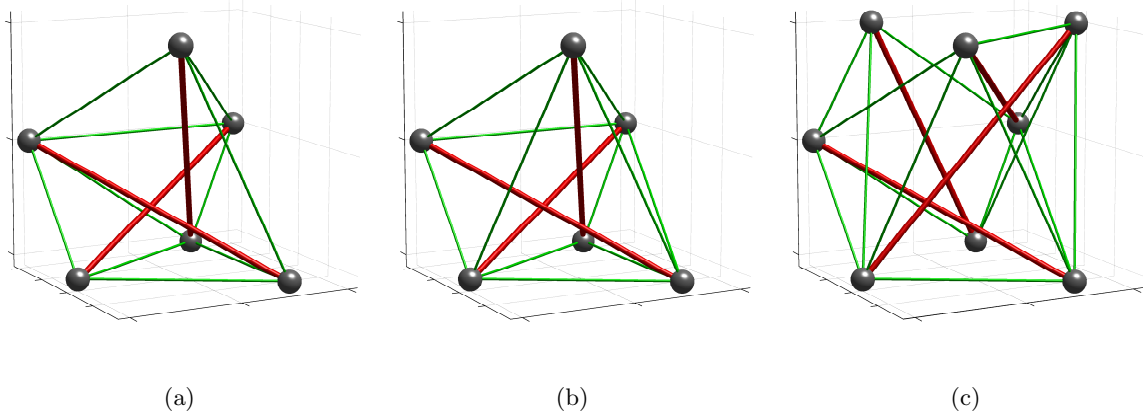


Figure 2: Optimal solutions obtained from the three-layer initial structure in Figure 1. An external force is applied at one of the top nodes. (a) the node at $(-1/2, -\sqrt{3}/2, 2)$ is loaded by a force $\hat{f} = 10$ N and $\bar{w} = 10$ J; (b) the node at $(-1/2, -\sqrt{3}/2, 2)$ is loaded by $\hat{f} = 200$ N and $\bar{w} = 10$ J; (c) the node at $(1, 0, 2)$ is loaded by $\hat{f} = 100$ N and $\bar{w} = 10$ J.

Table 1: Members of the solutions in Figure 2.

solution	$ S $	$ C $	d_s	d_k
(a)	3	10	1	0
(b)	3	11	2	0
(c)	4	15	1	0

pairs of intersecting members.

6.1.2 Solutions with single loaded node

We first examine cases in which only one of the top nodes of the structure is loaded.

Suppose that the node at $(-1/2, -\sqrt{3}/2, 2)$ is loaded by an external force $\hat{f} = 10$ N in the negative direction of the X_3 -axis. The upper bound for the compliance is $\bar{w} = 10$ J. As the optimal solution of the MILP problem (84), the structure depicted in Figure 2(a) is obtained. Here, the thick lines represent struts, while the thin lines represent cables. This tensegrity structure consists of 3 struts and 10 cables, as listed in Table 1. For a larger external load, $\hat{f} = 200$ N, we obtain the tensegrity structure shown in Figure 2(b). In Table 1, d_s and d_k represent the degrees of static indeterminacy and kinematic indeterminacy (after removing the degrees of rigid body motion), respectively. Thus, the solution in Figure 2(a) is kinematically determinate and has only one self-equilibrium mode of the axial forces. In contrast, the structure in Figure 2(b) has two self-equilibrium modes, one of which satisfies the definition of tensegrity in Definition 2.1.

Next, suppose that the node at $(1, 0, 2)$ is loaded by an external force $\hat{f} = 100$ N. Figure 2(c) shows the obtained solution, which includes 4 struts. Thus the optimal topology highly depends upon the loading condition. Note that all cables are in tension under the external forces in all the solutions obtained in this section.

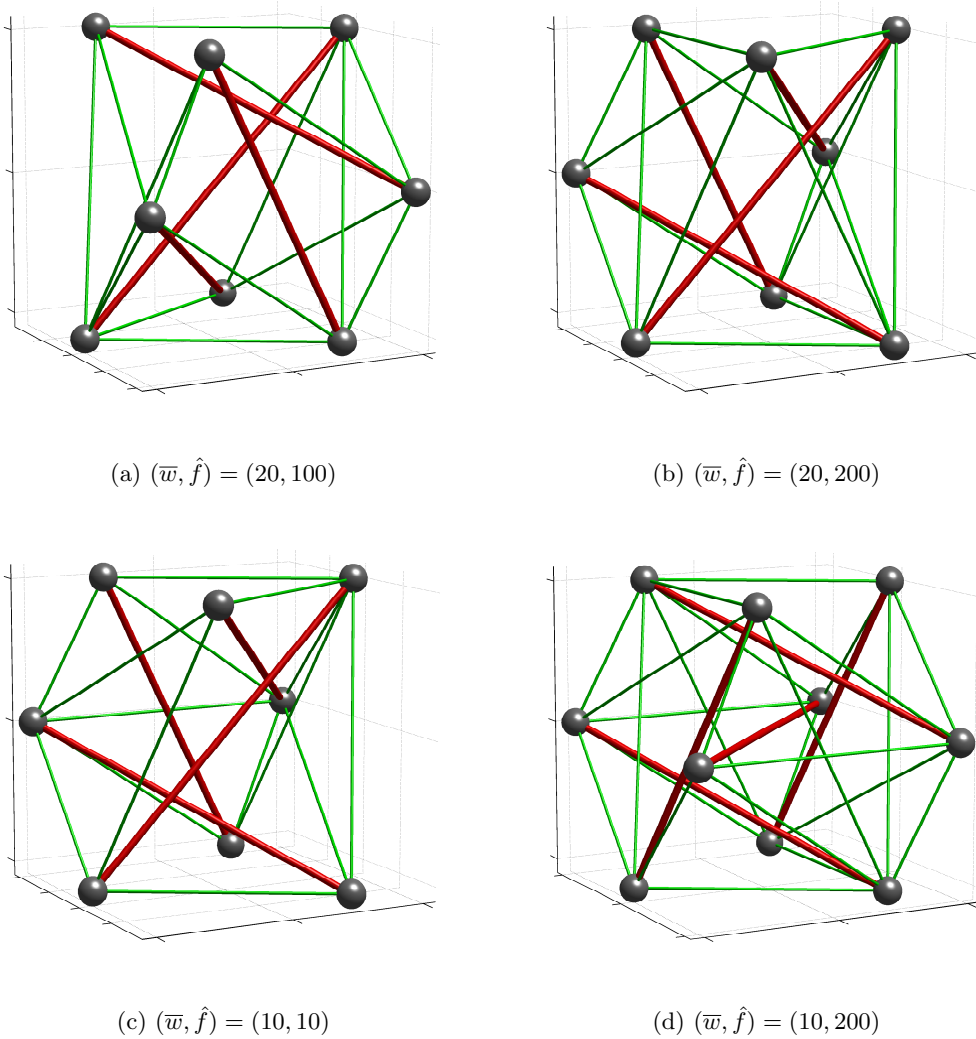


Figure 3: Optimal solutions obtained from the three-layer initial structure in Figure 1. External forces are applied at the three top nodes.

6.1.3 Solutions with three loaded node

We next examine the cases in which external forces are applied to all the nodes of the top triangular layer in Figure 1. The same force, denoted \hat{f} , is applied to every top node in the negative direction of the X_3 -axis.

We consider four cases: (a) $\bar{w} = 20$ J and $\hat{f} = 100$ N; (b) $\bar{w} = 20$ J and $\hat{f} = 200$ N; (c) $\bar{w} = 10$ J and $\hat{f} = 10$ N; and (d) $\bar{w} = 10$ J and $\hat{f} = 200$ N. The obtained tensegrity structures are shown in Figure 3. The computational results, as well as the numbers of struts and cables, are listed in Table 2. Here, w is the compliance of the optimal solution, “CPU” represents the computational time spent to solve the MILP problem (84) with CPLEX [13], and “Nodes” represents the number of visited nodes of the branch-and-bound tree. It is observed in Table 2 that as \hat{f} increases, the number of cables becomes larger. Accordingly, the number of self-equilibrium modes also becomes larger.

Among these four solutions, attention is focused on the structures in Figure 3(b) for $(\bar{w}, \hat{f}) =$

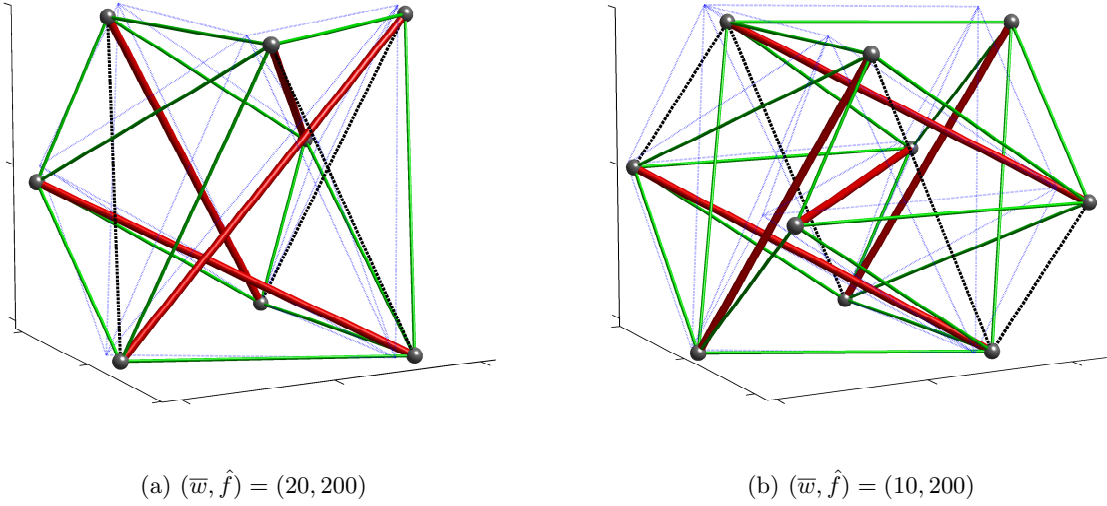


Figure 4: Equilibrium configurations of the solutions of the three-layer example. Cables in slack states are depicted with the dotted lines.

Table 2: Computational results of the solutions in Figure 3.

(\bar{w}, \hat{f})	$ S $	$ C $	d_s	d_k	w (J)	CPU (s)	Nodes
(20, 100)	4	15	1	0	19.929	12.4	2,871
(20, 200)	4	17	3	0	20.000	10.4	1,828
(10, 10)	4	15	1	0	0.822	27.1	4,463
(10, 200)	5	24	5	0	10.000	127.1	23,977

Table 3: Computational results of the five-layer example.

\bar{w} (J)	$ S $	$ C $	d_s	d_k	w (J)	CPU (s)	Nodes
80	7	29	1	1	73.13	63.0×10^3	3,121,218
50	7	31	2	0	47.82	242.1×10^3	9,604,988

(20, 200) and Figure 3(d) for $(\bar{w}, \hat{f}) = (10, 200)$. Some cables of these structures are in slack states at the equilibrium states under the external loads. The equilibrium configurations are as shown in Figure 4(a) (for the structure in Figure 3(b)) and in Figure 4(b) (for the structure in Figure 3(d)). The slack cables are depicted with dotted lines, where 3 cables are slack in Figure 4(a) and 4 cables are slack in Figure 4(b).

6.2 Inclined tensegrity structures

Two larger examples are presented, where the parameters such as the lower and upper bounds for axial forces are defined in a similar manner to section 6.1.1.

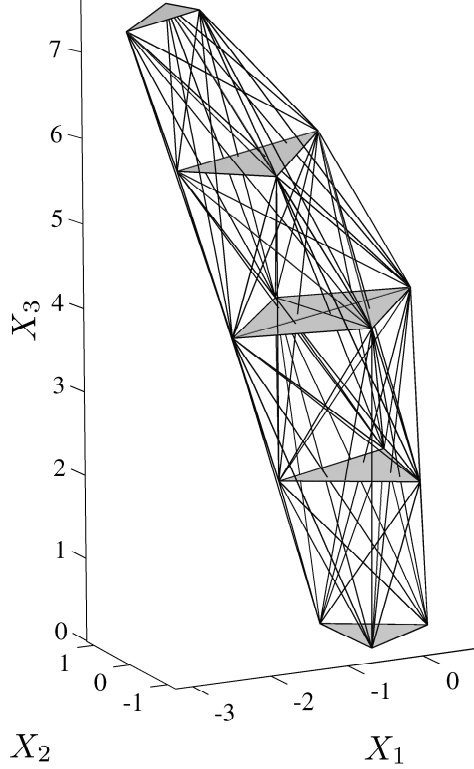


Figure 5: An initial structure with five layers.

Table 4: Maximal and minimal axial forces (in N) of the optimal solutions of the five-layer example.

	\bar{w} (J)	q_i ($i \in S$)	q_i ($i \in C$)	\tilde{s}_i ($i \in S$)	\tilde{s}_i ($i \in C$)
min	80	-1474.3	66.3	-1528.7	10.7
max	80	-567.4	931.8	-539.5	1000.0
min	50	-1435.4	60.4	-1516.4	0.0
max	50	-709.1	1000.0	-717.6	902.9

6.2.1 Five-layer tensegrity structures

Consider an initial structure illustrated in Figure 5. The structure consists of $|V| = 16$ nodes $|E| = 93$ members. The number of pairs of intersecting members is $|P_{\text{cross}}| = 32$.

The locations of the nodes of this initial structure are defined as follows. The nodes form five horizontal (but slightly inclined) layers, one of which is square and the others are equilateral triangles. We call these layers L_1, L_2, \dots, L_5 ; the bottom layer is L_1 , while the top layer is L_5 . The lengths of edges of L_1, \dots, L_5 are $3\sqrt{3}/4$ m, $\sqrt{3}$ m, $6\sqrt{2}/5$ m, $\sqrt{3}$ m, and $\sqrt{3}/2$ m, respectively. One of edges of L_1 is parallel with the X_2 -axis. First the layers are put horizontally, and their centers are on the X_3 -axis. The distance between the neighboring two layers is 2 m. The upper layer is rotated from the closest lower layer counter-clockwise around the X_3 -axis with the angle $\pi/4$. Accordingly, one of the edges of L_5 is parallel with the X_2 -axis. The diagonals of L_3 are

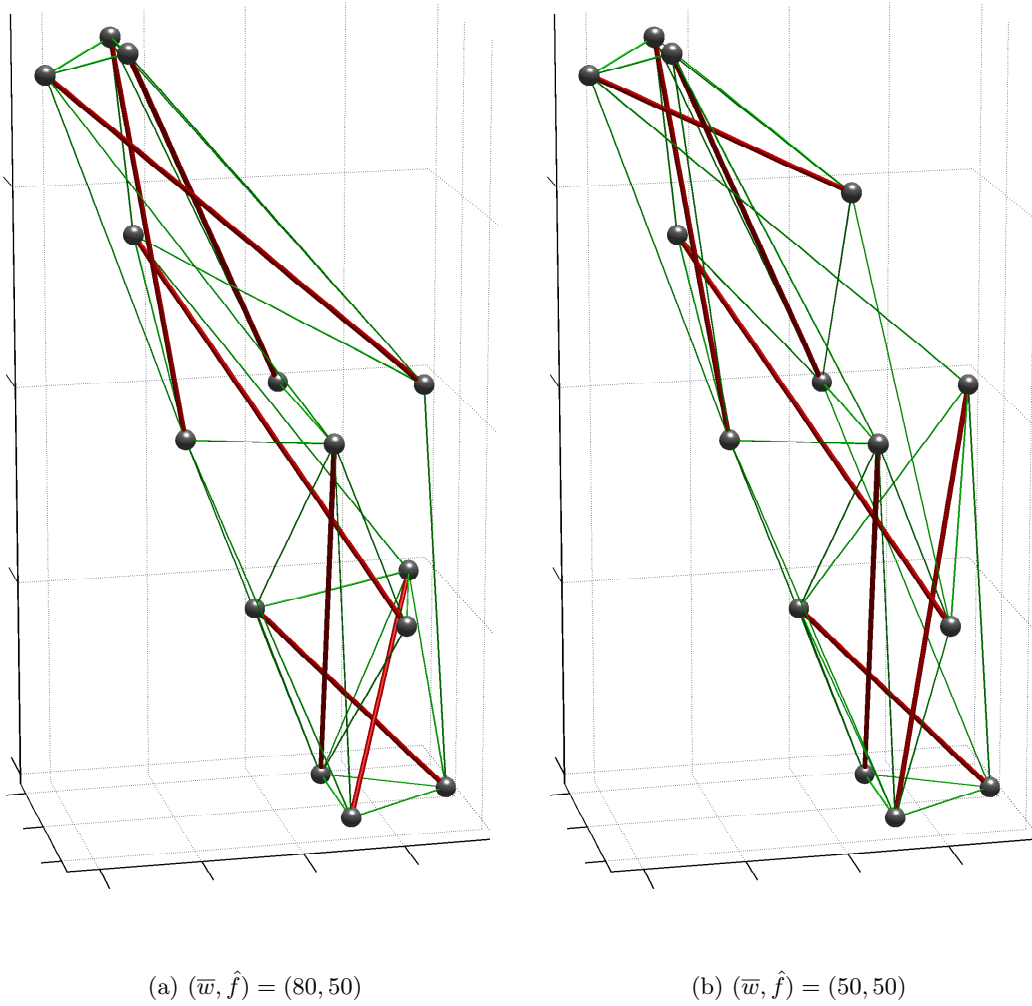


Figure 6: Optimal solutions of the five-layer example.

parallel with the X_1 - and the X_2 -axes. Then L_2, \dots, L_5 are rotated counter-clockwise around the X_2 -axis with the angles $5\pi/180$, $10\pi/180$, $15\pi/180$, and $20\pi/180$, respectively. Consequently, the locations of the nodes in Figure 5 are obtained. Any two nodes are connected by a member, but we remove members connecting the pairs $\{L_1, L_4\}$, $\{L_1, L_5\}$, and $\{L_2, L_5\}$.

Suppose that an external force $\hat{f} = 50$ N in the negative direction of the X_3 -axis is applied to each node on the top triangular layer. Displacements of the three bottom nodes are prescribed in the same manner as section 6.1.1. The optimal solutions obtained for $\bar{w} = 80$ J and $\bar{w} = 50$ J are shown in Figure 6. The numbers of struts and cables of these tensegrity structures, as well as the computational results, are listed in Table 3.

The locations of the struts, as well as the cables, are different between the two tensegrity structures in Figure 5. Two nodes of the initial structure in Figure 5 are not used in each of these tensegrity structures. The maximal and minimal member axial forces of struts and cables are listed in Table 4, where q_i is the prestress and \tilde{s}_i is the axial force at the equilibrium state in the presence of the external load. It is worth of noting that one cable of the structure in Figure 6(b) is in a slack state under the external load. The equilibrium configuration is shown in Figure 7.

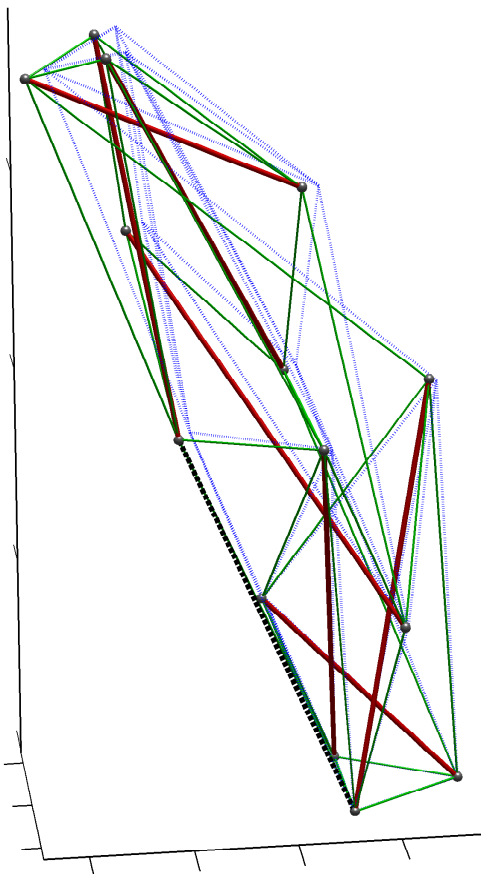


Figure 7: Equilibrium configurations of the solution of the three-layer example with $(\bar{w}, \hat{f}) = (50, 50)$. Cables in slack states are depicted with the dotted lines.

Table 5: Computational results of the six-layer example.

\bar{w} (J)	w (J)	CPU (s)	Nodes
30	28.93	67.0×10^3	1,940,065
20	19.66	46.6×10^3	1,577,438

6.2.2 Six-layer tensegrity structures

We next consider an initial structure illustrated in Figure 8. This structure consists of $|V| = 18$ nodes $|E| = 99$ members. The number of pairs of intersecting members is $|P_{\text{cross}}| = 18$.

The locations of the nodes are defined in a manner similar to section 6.2.1. The nodes form six equilateral triangles as shown in Figure 8. These triangles are called L_1, L_2, \dots, L_6 , where the bottom one is L_1 and the top one is L_6 . The lengths of edges of L_1, \dots, L_6 are $\sqrt{3}$ m, $\sqrt{3}$ m, $6\sqrt{2}/5$ m, $\sqrt{3}$ m, $4\sqrt{3}/5$ m, and $\sqrt{3}/2$ m, respectively. One of edges of L_1 is parallel with the X_2 -axis. We first arrange the triangles horizontally. Their centers are on the X_3 -axis, and the distance between each pair of neighboring triangles is 1.5 m. The upper layer is rotated from the closest lower layer counter-clockwise around the X_3 -axis with the angle $\pi/4$. Accordingly, one of the edges of L_5 is parallel with the X_2 -axis. Then L_2, \dots, L_6 are rotated counter-clockwise around

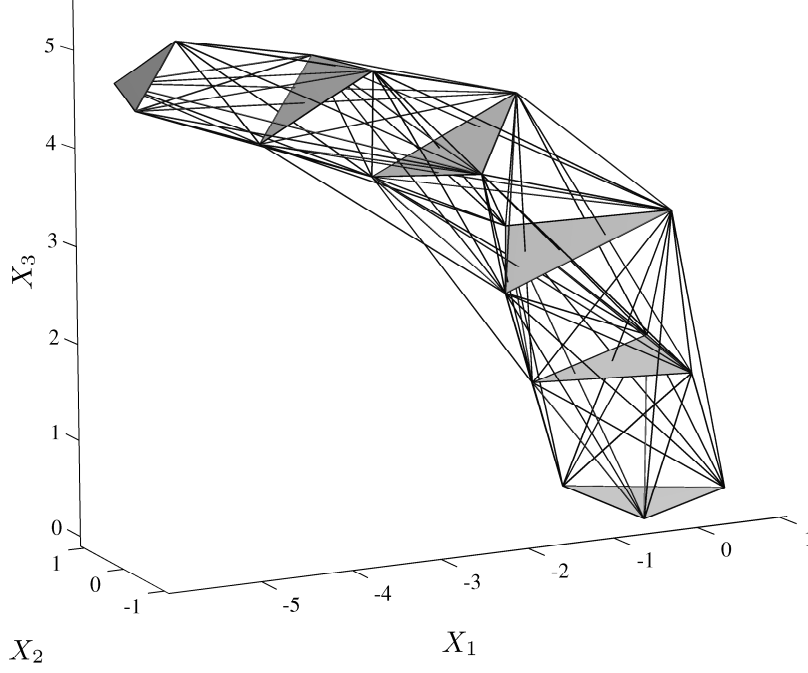


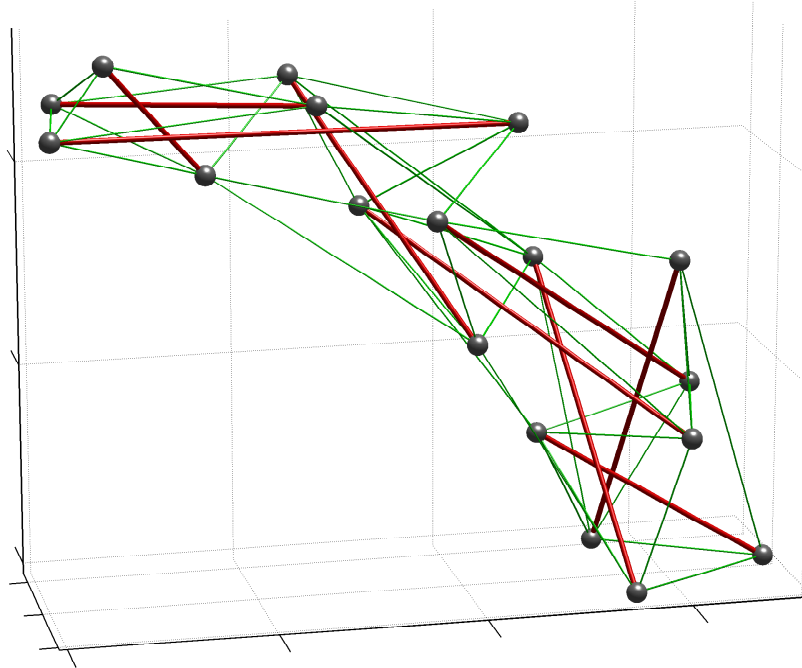
Figure 8: An initial structure with six layers.

Table 6: Maximal and minimal axial forces (in N) of the optimal solutions of the six-layer example.

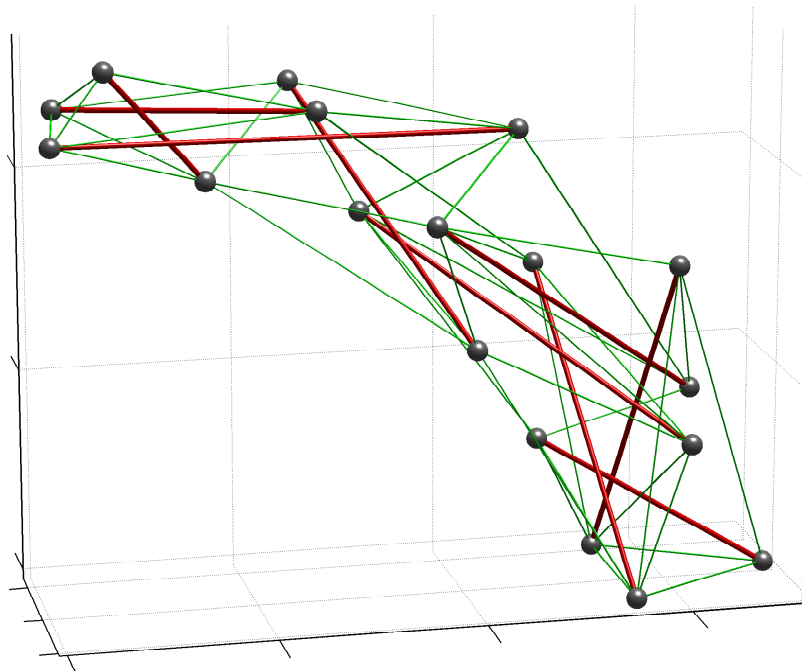
	\bar{w} (J)	q_i ($i \in S$)	q_i ($i \in C$)	\tilde{s}_i ($i \in S$)	\tilde{s}_i ($i \in C$)
min	30	-1735.2	53.6	-1709.6	32.5
max	30	-722.6	1000.0	-706.8	971.9
max	20	-1861.3	50.6	-1875.5	24.2
min	20	-592.3	994.2	-617.8	1000.0

the X_2 -axis with the angles $10\pi/180$, $20\pi/180$, $30\pi/180$, $40\pi/180$, and $50\pi/180$, respectively. To avoid existence of too long members, members connecting the pairs $\{L_1, L_4\}$, $\{L_1, L_5\}$, $\{L_1, L_6\}$, $\{L_2, L_5\}$, $\{L_2, L_6\}$, and $\{L_3, L_6\}$ are not considered. All the other members connecting two nodes are considered as candidate members.

An external force $\hat{f} = 10$ N in the negative direction of the X_3 -axis is applied to each of the top three nodes. To avoid the rigid body motion, the displacements of the three bottom nodes are fixed in the same manner as section 6.1.1. Regarding the upper bound for the compliance, we consider two cases, say, $\bar{w} = 30$ J and $\bar{w} = 20$ J. As the optimal solutions, we obtain the tensegrity structures illustrated in Figure 9. The computational results are listed in Table 5. The maximal and minimal axial forces of cables and struts are listed in Table 6, from which we can see that no cable is in a slack state. Note that the locations of cables are different between these tensegrity structures, while the locations of struts are same. Both the tensegrity structures have $|S| = 9$ struts and $|C| = 40$ cables, have only one self-equilibrium mode, and are kinematically determinate. Thus, compared with Figure 9(a), the compliance is improved (i.e., decreased) in Figure 9(b) by changing the locations of cables.



(a) $(\bar{w}, \hat{f}) = (30, 10)$



(b) $(\bar{w}, \hat{f}) = (20, 10)$

Figure 9: Optimal solutions of the six-layer example.

7 Conclusions

In finding new topologies of tensegrity structures, the difficulty primarily stems from the discontinuity condition of struts. In this paper, this difficulty is dealt with in the framework of mixed integer linear programming (MILP). It has been shown that the topology optimization of tensegrity structures under the stress constraints and the compliance constraint can be formulated as an MILP problem. As the global optimal solutions of this problem, various configurations of tensegrity structures have been obtained throughout the numerical experiments.

This paper has developed a method for optimizing topology of tensegrity structures without requiring any connectivity information of cables and struts as input data. Much remains to be explored. Other optimization problems for tensegrity structures can be formulated to find real-life functional tensegrity structures. For instance, in the presented approach, the member cross-sectional areas and the locations of nodes have not been considered as design variables. Also, the geometrical nonlinearity has not been addressed. Furthermore, the proposed formulation results in a large MILP problem, which might be a potential disadvantage for finding tensegrity structures consisting of a large number of members from a view point of computational efforts.

Acknowledgments

This work is supported in part by a Grant-in-Aid for Scientific Research from the Ministry of Education, Culture, Sports, Science and Technology of Japan.

References

- [1] Achtziger, W., Stolpe, M.: Truss topology optimization with discrete design variables—guaranteed global optimality and benchmark examples. *Structural and Multidisciplinary Optimization*, **34**, 1–20 (2007).
- [2] Adam, B., Smith, I.F.C.: Active tensegrity: a control framework for an adaptive civil-engineering structure. *Computers & Structures*, **86**, 2215–2223 (2008).
- [3] Atai, A.A., Steigmann, D.J.: On the nonlinear mechanics of discrete networks. *Archive of Applied Mechanics*, **67**, 303–319 (1997).
- [4] Baudriller, H., Maurin, B., Cañadas, P., Montcourrier, P., Parmeggiani, A., Bettache, N.: Form-finding of complex tensegrity structures: Application to cell cytoskeleton modelling. *Comptes Rendus Mécanique*, **334**, 662–668 (2006)
- [5] Bel Hadj Ali, N., Rhode-Barbarigos, L., Pascual Albi, A.A., Smith, I.F.C.: Design optimization and dynamic analysis of a tensegrity-based footbridge. *Engineering Structures*, **32**, 3650–3659 (2010).
- [6] Connelly, R., Back, A.: Mathematics and tensegrity. *American Scientist*, **86**, 142–151 (1998).
- [7] Connelly, R., Terrell, M.: Globally rigid symmetric tensegrities. *Structural Topology*, **21**, 59–77 (1995).

- [8] Deng, H., Jiang, Q.F., Kwan, A.S.K.: Shape finding of incomplete cable-strut assemblies containing slack and prestressed elements. *Computers & Structures*, **83**, 1767–1779 (2005).
- [9] Djouadi, S., Motro, R., Pons, J.C., Crosnier, B.: Active control of tensegrity systems. *Journal of Aerospace Engineering (ASCE)*, **11**, 37–44 (1998).
- [10] Ehara, S., Kanno, Y.: Topology design of tensegrity structures via mixed integer programming. *International Journal of Solids and Structures*, **47**, 571–579 (2010).
- [11] Fuller, R.B.: *Synergetics: Explorations in the Geometry of Thinking*. Collier McMillian, London (1975).
- [12] Gomez Estrada, G., Bungartz, H.-J., Mohrdieck, C.: Numerical form-finding of tensegrity structures. *International Journal of Solids and Structures*, **43**, 6855–6868 (2006).
- [13] IBM ILOG: *User’s Manual for CPLEX*. <http://www.ilog.com>.
- [14] Jórdan, T., Recski, A., Szabadka, Z.: Rigid tensegrity labelings of graphs. *European Journal of Combinatorics*, **30**, 1887–1895 (2009).
- [15] Juan, S.H., Mirats Tur, J.M.: Tensegrity frameworks: static analysis review. *Mechanism and Machine Theory*, **43**, 859–881 (2008).
- [16] Kanno, Y.: *Nonsmooth Mechanics and Convex Optimization*. CRC Press, Boca Raton (2011).
- [17] Kanno, Y., Guo, X.: A mixed integer programming for robust truss topology optimization with stress constraints. *International Journal for Numerical Methods in Engineering*, **83**, 1675–1699 (2010).
- [18] Li, Y., Feng, X.-Q., Cao, Y.-P., Gao, H.: A Monte Carlo form-finding method for large scale regular and irregular tensegrity structures. *International Journal of Solids and Structures*, **47**, 1888–1898 (2010).
- [19] Masic, M., Skelton, R.E., Gill, P.E.: Algebraic tensegrity form-finding. *International Journal of Solids and Structures*, **42**, 4833–4858 (2005).
- [20] Masic, M., Skelton, R.E., Gill, P.E.: Optimization of tensegrity structures. *International Journal of Solids and Structures*, **43**, 4687–4703 (2006).
- [21] Micheletti, A., Williams, W.O.: A marching procedure for form-finding for tensegrity structures. *Journal of Mechanics of Materials and Structures*, **2**, 857–882 (2007).
- [22] Motro, R.: *Tensegrity*. Kogan Page Science, London (2003).
- [23] Murakami, H.: Static and dynamic analyses of tensegrity structures, part 1: nonlinear equations of motion. *International Journal of Solids and Structures*, **38**, 3599–3613 (2001).
- [24] Murakami, H., Nishimura, Y.: Initial shape finding and modal analyses of cyclic right-cylindrical tensegrity modules. *Computers & Structures*, **79**, 891–917 (2001).

- [25] Ohsaki, M., Katoh, N.: Topology optimization of trusses with stress and local constraints on nodal stability and member intersection. *Structural and Multidisciplinary Optimization*, **29**, 190–197 (2005).
- [26] Pagitz, M. Mirats Tur, J.M.: Finite element based form-finding algorithm for tensegrity structures. *International Journal of Solids and Structures*, **46**, 3235–3240 (2009).
- [27] Panagiotopoulos, P.D.: Stress-unilateral analysis of discretized cable and membrane structure in the presence of large displacements. *Ingenieur-Archiv*, **44**, 291–300 (1975).
- [28] Rasmussen, M.H., Stolpe, M.: Global optimization of discrete truss topology design problems using a parallel cut-and-branch method. *Computers & Structures*, **86**, 1527–1538 (2008).
- [29] Rieffel, J., Valero-Cuevasa, F., Lipson, H.: Automated discovery and optimization of large irregular tensegrity structures. *Computers & Structures*, **87**, 368–379 (2009).
- [30] Stamenović, D., Coughlin, M.F.: A quantitative model of cellular elasticity based on tensegrity. *Journal of Biomechanical Engineering (ASME)*, **122**, 39–43 (2000).
- [31] Stolpe, M., Svanberg, K.: Modelling topology optimization problems as linear mixed 0–1 programs. *International Journal for Numerical Methods in Engineering*, **57**, 723–739 (2003).
- [32] Sultan, C., Corless, M., Skelton, R.: Symmetrical reconfiguration of tensegrity structures. *International Journal of Solids and Structures*, **39**, 2215–2234 (2002).
- [33] Sultan, C., Skelton, R.: Deployment of tensegrity structures. *International Journal of Solids and Structures*, **40**, 4637–4657 (2003).
- [34] Sultan, C., Skelton, R.: A force and torque tensegrity sensor. *Sensors and Actuators A: Physical*, **112**, 220–231 (2004).
- [35] Tibert, A.G., Pellegrino, S.: Deployable tensegrity reflectors for small satellites. *Journal of Spacecraft and Rockets (AIAA)*, **39**, 701–709 (2002).
- [36] Tibert, A.G., Pellegrino, S.: Review of form-finding methods for tensegrity structures. *International Journal of Space Structures*, **18**, 209–223 (2003).
- [37] Tran, H.C., Lee, J.: Advanced form-finding for cable-strut structures. *International Journal of Solids and Structures (AIAA)*, **47**, 1785–1794 (2010).
- [38] Volokh, K.Yu., Vilnay, O., Belsky, M.: Tensegrity architecture explains linear stiffening and predicts softening of living cells. *Journal of Biomechanics*, **33**, 1543–1549 (2000).
- [39] Wandling, S., Cañadas, P., Chabrand, P.: Towards a generalised tensegrity model describing the mechanical behaviour of the cytoskeleton structure. *Computer Methods in Biomechanics and Biomedical Engineering*, **6**, 45–52 (2003).
- [40] Zhang, J.Y., Ohsaki, M.: Adaptive force density method for form-finding problem of tensegrity structures. *International Journal of Solids and Structures*, **43**, 5658–5673 (2006).

- [41] Zhang, J.Y., Ohsaki, M., Kanno, Y.: A direct approach to design of geometry and forces of tensegrity systems. *International Journal of Solids and Structures*, **43**, 2260–2278 (2006).